Analysis of transmission through small apertures in conducting films

K. J. Webb* and J. Li
School of Electrical and Computer Engineering, Purdue University, 465 Northwestern Avenue, West Lafayette, Indiana 47907-2035, USA
(Received 15 August 2005; published 5 January 2006)

The transmission characteristics of small slots and circular apertures in conducting films are described using a waveguide mode analysis and numerical simulations. A set of modes are shown to exist for a circular waveguide hole which propagate for an arbitrarily small diameter. As the hole becomes small, loading with a dielectric allows for low loss over a significant wavelength range.

DOI: 10.1103/PhysRevB.73.033401 PACS number(s): 78.66.Bz, 42.79.Ag, 42.79.Gn, 71.36.+c

Efficient coupling of electromagnetic fields through very small apertures in conducting films could lead to dramatic improvements in fields such as optical lithography in semiconductor processing, data storage, and imaging. Experimental results showing what appeared to be increased transmission over what might be expected through an array of subwavelength apertures therefore created significant excitement.[1] Consequently, a large number of papers have been published dealing with aperture arrays,[2–5] single apertures with periodic grooves,[6–8] and single apertures in a smooth metal film.[9]

Two-dimensional (2D) slots in metal films can have a propagating mode (at optical wavelengths) for an arbitrarily small slot width.[10–13] While metal-walled circular waveguides have been studied (see the case of Al,[14] lossless metals,[15] and near field scanning optical microscope models[16]), it has generally been widely accepted that with a sufficiently small radius, there will be no propagating modes, i.e., the loss will be high, and the dominant coupling mechanism will be through decaying fields. We show that, in fact, there are a set of modes which can propagate in arbitrarily small circular holes with appropriate material parameters. While there are fabrication challenges, this opens up a regime of application prospects.

For an infinitesimally thin conductor, the use of approximate electric and magnetic equivalent dipole sources over the aperture support, which are proportional to the fields with the aperture closed, provided Bethe an approximate analysis for small hole coupling.[17] A more exact analysis requires a numerical electromagnetics solution. One approach is to represent the field solution inside a uniform cross-section cylindrical hole by means of the waveguide eigenmode set, and to couple this field to those in the semi-infinite half-spaces on either side. Describing the waveguide properties is thus important in understanding the transmission through small holes.

We treat the 2D lossy eigenmode problem first, showing that multiple resonances in a single dominant mode support the numerical simulations. Then we solve the circular hole eigenvalue problem, showing an important class of modes. The geometry we consider is shown in Fig. 1, where the 2D slot has a width $2a$ and the circular hole has a diameter $2a$. Throughout we assume a bulk metal complex dielectric constant. With geometries small relative to the screening length, a more sophisticated description of the material is needed.[18] We assume that the material in the hole is lossless.

Figure 2 shows a finite element simulation of coupling through a $2a=4$ nm wide slot in a $b=56.3$ nm thick Ag film with a normally incident plane wave (H_y, E_x, E_z, or a TM mode in waveguide nomenclature) in free space from the top having a wavelength $\lambda_0=582$ nm. The film modeled had a finite width of 198 nm and perfectly conducting shielding elements at the ends to prevent surface wave coupling around the structure to the back side, allowing us to create an effective near-field model for a single slot in a wide metal film. In the case shown, b was adjusted for resonance in a propagating mode that exists for small a. An integral equation solution has shown transmission peaks which depend on the wavelength, and this has been explained as being due to an interfering surface-wave-type mode in the slot.[13] We show that the mode responsible is the lowest order TM mode which decays away from both surfaces of this slot, and that this single mode can explain the multiple transmission peaks as the slot length is varied. We also establish that the loss is acceptable at currently conceivable fabrication dimensions.

The waveguide mode eigenvalues can be determined from the transverse resonance condition in the slot using

$$Z_{x1}\frac{Z_{x2}+Z_{x1}\tanh(-ik_{x1}a)}{Z_{x1}+Z_{x2}\tanh(-ik_{x1}a)}\rightarrow\begin{cases}0\\ \infty\end{cases}, \tag{1}$$

where a zero result is the case of an electric wall (minimum tangential electric field) at $x=0$, the infinite case is for a magnetic wall (minimum tangential magnetic field), and Z_x is the x-directed wave impedance. From the dispersion relation, $k_{xi}^2=k_i^2-k_z^2$, with the imposition of $k_{z1}=k_{z2}=k_z$, where $k_i^2=(\omega/c)^2\epsilon_i$, with ϵ_1 the real dielectric constant for the slot and ϵ_2 the complex value for the metal. For the TM case, $Z_{xi}=k_{xi}/(\omega\epsilon_i\epsilon_0)$, where ϵ_0 is the permittivity of free space. The TM modes with an electric wall at $x=0$ are excited by the

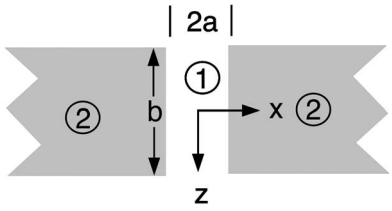

FIG. 1. The 2D ($2a$ is width) slot and 3D (a is radius) hole geometry.

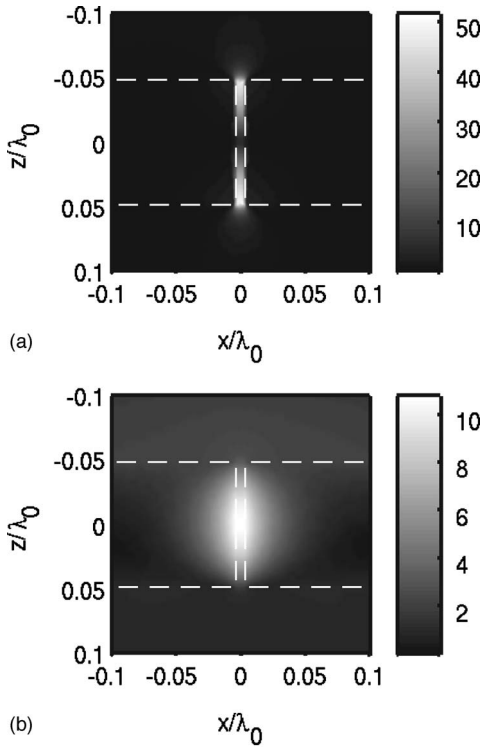

FIG. 2. TM field solution for a 2D slot: (a) $|E_x|$ normalized to the incident field and (b) normalized $|H_y|$. The parameters are $\epsilon_2=-14.88+i0.39$, $2a=4$ nm, $b=56.3$ nm, and $\lambda_0=582$ nm.

incident plane wave in the solution of Fig. 2. We solve for the complex eigenvalues using nonlinear optimization with initial values corresponding to the lossless eigenvalues. The results for $k_z=\beta_z+i\alpha_z$ with four ϵ_2/ϵ_1 values are given in Fig. 3 as a function of normalized slot half-width (a/λ_1), where $\lambda_1=2\pi/k_1$. With a view to dispersion, the physically meaningful interpretation of a/λ_1 is a scaled dimension. With $\epsilon_1=1$, the ϵ_2 values selected correspond to the dielectric constant for Ag at wavelengths of 331.5 nm ($\epsilon_2=-0.66+i0.28$), 354 nm ($\epsilon_2=-2.00+i0.28$), 582 nm ($\epsilon_2=-14.88+i0.39$), and 1.088 μm ($\epsilon_2=-60.76+i0.62$).[19] Only the lowest order modes which do not have a cut-off frequency are shown. These modes have fields decaying away from both

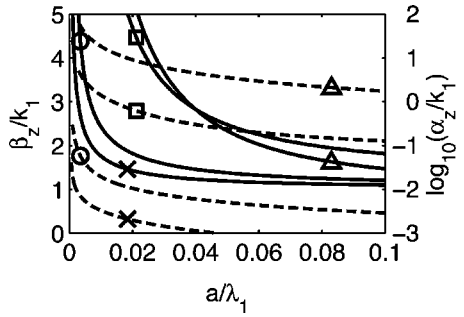

FIG. 3. Normalized slot dispersion curves for $k_z/k_1=(\beta_z+i\alpha_z)/k_1$. The solid lines show β_z/k_1 and the dashed lines $\log_{10}(\alpha_z/k_1)$ for: $\epsilon_2/\epsilon_1=-60.76+i0.62$ (crosses); $\epsilon_2/\epsilon_1=-14.88+i0.39$ (circles); $\epsilon_2/\epsilon_1=-2.00+i0.28$ (squares); $\epsilon_2/\epsilon_1=-0.66+i0.28$ (triangles).

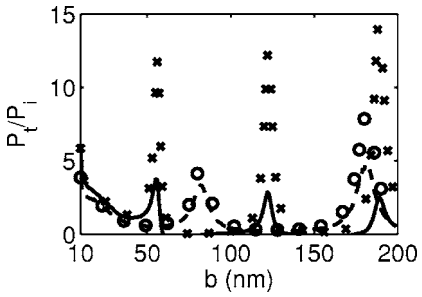

FIG. 4. Normalized power transmission (P_t/P_i) through a 2D slot as a function of thickness. Parameters: $\epsilon_{r2}=-14.88+i0.39$ (Ag at $\lambda_0=582.08$ nm), $\epsilon_1=1$, $2a=4$ nm (solid line), and $2a=8$ nm (dashed line). The symbols show the result for the top of the slot and the solid and dashed lines for the bottom of the slot.

sides of both interfaces in the slot, and $\beta_z/k_1>1$.[10] The propagating slot mode is similar to a surface mode as the slot becomes wide, but has two symmetries (electric and/or magnetic wall at $x=0$). The surface mode eigenvalues are given by $Z_{x1}=-Z_{x2}$ [$a\to\infty$ in (1)], leading to $k_z/k_1=\sqrt{(\epsilon_2/\epsilon_1)/(1+\epsilon_2/\epsilon_1)}$. For a propagating surface mode in the lossless case, $\epsilon_2/\epsilon_1<-1$, a requirement which does not apply for the slot case. The slot mode attenuation increases as a is reduced[11] and, for a fixed ϵ_2, as ϵ_1 is increased.[12] However, the loss can be acceptable even for extremely small slot widths. At $\lambda_0=582$ nm and for $2a=4$ nm, the attenuation (from Fig. 3) is 0.005 dB/nm for $\epsilon_1=1$ and 0.014 dB/nm for $\epsilon_1=2.13$ (SiO_2, glass[20]). The 2D slot thus provides virtually arbitrarily small one-dimensional spatial resolution.

The results from a series of finite element simulations for power transfer through a small 2D slot ($\epsilon_1=1$) in a Ag film with varying thickness (b) is shown in Fig. 4. Two slot widths are considered, 4 and 8 nm. The power passing through the aperture is P_t and that due to the incident field Poynting vector with area (width) equal to the slot cross-section results in P_i. The solid and dashed lines are the cases for P_t calculated at the bottom of the slot, and the symbols give the result for the power passing through the aperture at the top of the slot. Notice the periodic resonant features with varying slot lengths (metal thickness) and the correspondingly large P_t/P_i. Using the single propagating mode eigenvalue from Fig. 3, the resonance peaks in Fig. 4 are spaced at multiples of $\lambda_z/2$ ($=\pi/\beta_z$). The difference between the power through the top and the bottom aperture of the slot is primarily due to dissipation.

Now consider Fig. 1 as a circular cylindrical hole through a metal film having a complex dielectric constant (ϵ_2), and a lossless material in the aperture (ϵ_1). The eigenmodes are available from a solution to the Helmholtz wave equation in cylindrical coordinates.[21] Applying boundary conditions on the tangential fields at $r=a$ leads to

$$\left[\frac{I_l'(pa)}{paI_l(pa)}-\frac{K_l'(qa)}{qaK_l(qa)}\right]\left[\frac{I_l'(pa)}{paI_l(pa)}-\frac{\epsilon_2K_l'(qa)}{\epsilon_1qaK_l(qa)}\right]=l^2\left(\frac{k_z}{k_1}\right)^2\left[\left(\frac{1}{pa}\right)^2-\left(\frac{1}{qa}\right)^2\right]^2, \quad (2)$$

where $p=\sqrt{k_z^2-k_1^2}$, $q=\sqrt{k_z^2-k_2^2}$, and a is the aperture radius. In

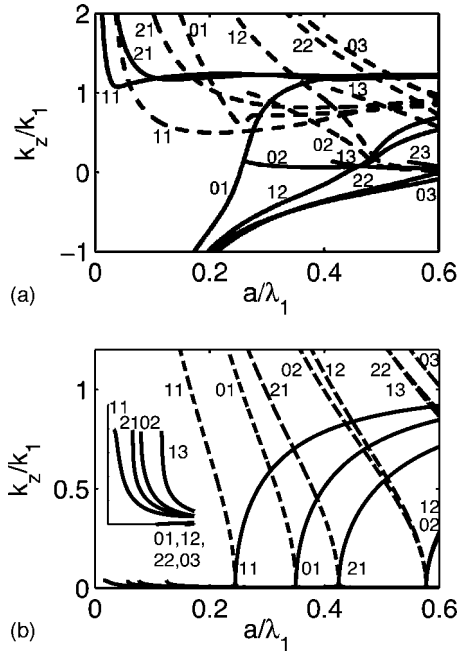

FIG. 5. Circular waveguide dispersion curves for $k_z/k_1=(\beta_z+i\alpha_z)/k_1$: (a) $\epsilon_2/\epsilon_1=-0.90+i0.30$; (b) $\epsilon_2/\epsilon_1=-23.41+i0.39$. The lj indices indicate the jth root of the l mode. The solid lines are for β_z/k_1 and the dashed lines are for α_z/k_1. The inset in (b) shows β_z for small a/λ_1 near the termination points.

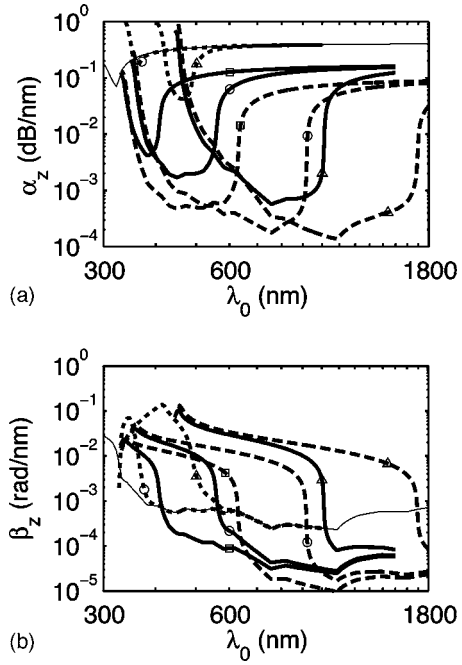

FIG. 6. Circular waveguide 11 mode attenuation (a) and phase constant (b) for a Ag film with $a=10$ nm (short dashed line), $a=75$ nm (thick solid line), and $a=150$ nm (long dashed line). The square symbol indicates $\epsilon_1=1$, a circle $\epsilon_1=2.16$, and a triangle $\epsilon_1=7.46$. The thin solid line gives the result for bulk Ag.

Eq. (2), $I_l(\ )$ is the modified Bessel function of the first kind of integer order l, and for $p=-ih$, $I_l(-ih)=(i)^{-l}J_l(h)$, where $J_l(\ )$ is the Bessel function of the first kind, and $K_l(\ )$ is the modified Bessel function of the second kind. The prime in Eq. (2) indicates a derivative defined by $I_l'(pa)=\partial I_l(pr)/\partial(pr)|_{r=a}$.

There are TM (E_z,E_r,H_ϕ) and TE (H_z,H_r,E_ϕ) solutions to Eq. (2) for $l=0$, and a set of hybrid solutions having all six field components $(l\geqslant 1)$ which are EH (TM-like) and HE (TE-like). We denote a set of solutions $j=1,2,\ldots$, for each $l=0,1,2,\ldots$, resulting in an lj index. With no loss, solutions exist in domains $k_z/k_1>1$ and $k_z/k_1<1$. It is instructive to consider two parameter regimes, $-1<\epsilon_2/\epsilon_1<0$ and $\epsilon_2/\epsilon_1<-1$. With $-1<\epsilon_2/\epsilon_1<0$, we find a set of propagating modes having $k_z/k_1>1$ that exist for arbitrarily small a/λ_1 $(l=1,2)$, as noted before.[15] There is also a mode set confined to $k_z/k_1<1$ having imaginary $p=-ih$. In the second parameter regime, with $\epsilon_2/\epsilon_1<-1$, all modes have a cut-off. One solution set has a real p and a large argument $(a/\lambda_1\rightarrow\infty)$ asymptote as in the surface-wave case. The other has an imaginary $p=-ih$ and is constrained by $k_z/k_1<1$. From a lossless eigenmode solution with a Drude model, allowing a convenient analysis as a function of frequency, it has been suggested that when $\epsilon_2/\epsilon_1\approx-1$ a propagation mode can be found regardless of how small the hole.[22] The correct dispersion curves require the incorporation of loss, i.e., the solution of the complex eigenvalue problem. We show these lossy waveguide solutions, proving that in fact a propagating mode does exist for arbitrarily small holes, and demonstrate that these solutions encompass a range of ϵ_2/ϵ_1.

Figure 5 shows normalized solutions of Eq. (2), k_z/k_1, as a function of normalized hole radius, for (i) $\epsilon_2/\epsilon_1=-0.9+i0.30$ (Ag at $\lambda=335.8$ nm,[19] with $\epsilon_1=1$), and (ii) $\epsilon_2/\epsilon_1=-23.41+i0.39$ (Ag at $\lambda=704.4$ nm,[19] with $\epsilon_1=1$). Well behaved solutions require $\mathrm{Re}\{q\}\geqslant 0$, where Re refers to the real part, and dispersion curves terminate on the condition $\mathrm{Re}\{q\}=0$. The 11 mode dominates, as it has the lowest loss; it is EH for case (i) and HE for case (ii). Interestingly, for case (i), the TM and EH modes shown (except the 11 and 21 modes) pass from positive to negative β_z/k_1 as a/λ_1 is reduced, while the TE and HE modes have increasingly positive β_z/k_1. In all cases, the Poynting vector remains positive. Our result shows that with the introduction of loss, the dispersion curves no longer have two values, as suggested in an earlier work dealing with the lossless problem.[15] The 01, 11, 21, 12, 22, and 03 (TM and EH) modes do not terminate and hence propagate for arbitrarily small a/λ_1, with the 11 mode having the lowest loss. For case (ii) and small a/λ_1, the decaying 11 mode may not terminate, as noted in earlier work,[14] (but the attenuation becomes high; this is also the mode emphasized in a recent lossless study[22]).

While Fig. 5 shows that the waveguide mode loss increases with decreasing a/λ_1, this can be controlled through ϵ_1, along with the wavelength range for suitable operation. Figure 6(a) illustrates the 11 mode loss for a Ag film[19] as a function of the incident free space wavelength (λ_0) for $a=10$, 75, and 150 nm and material in the aperture having $\epsilon_1=1,2.16$ (SiO_2,[20] assumed independent of λ_0), and 7.46 (SiC,[20] also assumed independent of λ_0). Clearly the larger hole has a lower loss, and increasing ϵ_1 moves the low loss regime to longer wavelengths. Using an attenuation change from the minimum of 10^{-2} dB/nm as a measure of a band-

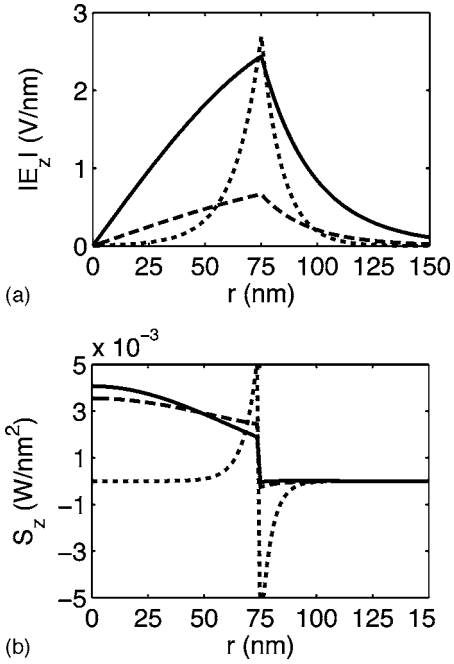

FIG. 7. (a) Electric field magnitude $|E_z(r)|$ and (b) Poynting vector $S_z(r)$ for a Ag film with $a=75$ nm and $\lambda_0=450$ nm. The solid line is for $\epsilon_1=1$, the long dashed line for $\epsilon_1=2.16$, and the short dashed line is for $\epsilon_1=7.46$. The data for the solid line and the long dashed line cases have been multiplied by 10 in (a) and 50 in (b).

width, the case for $a=75$ nm and $\epsilon_1=2.16$ has a bandwidth of about 200 nm, and for $\epsilon_1=1$, the bandwidth is about 100 nm. Even for $a=10$ nm and $\epsilon_1=7.46$, the loss is less than that in bulk Ag (Ref. 19) over a 100 nm band. However, with $a=10$ nm and $\epsilon_1=1, 2.16$, the attenuation is virtually the same as the bulk Ag, so even though the waveguide mode has confined fields, this relatively high loss will prevent effective coupling though the hole. Note that with $a=75$ nm and $\epsilon_1=1$, the case of earlier experiments,[1] the 11 mode propagates. Also note that the $a=10$ nm case with $\epsilon_1=7.46$ has an order or magnitude lower loss than bulk Ag for a parameter space that includes $\mathrm{Re}\{\epsilon_2/\epsilon_1\}>-1$.

To explore the waveguide field confinement further, we show the longitudinal electric field and Poynting vector (S_z) in Fig. 7 for circular waveguide in Ag (with material parameters $\epsilon_2=-7.02+i0.21$)[19] having $a=75$ nm and $\lambda_0=450$ nm. The solid line is for $\epsilon_1=1$ and $k_z/k_0=k_z/k_1=0.01+i0.63$, the long dashed line is for $\epsilon_1=2.16$ and $k_z/k_0=1.13+i0.01$ ($k_z/k_1=0.77+i0.01$), and the short dashed line is for $\epsilon_1=7.46$ and $k_z/k_0=6.87+i4.98$ ($k_z/k_1=2.52+i1.82$). The field and Poynting vector are normalized for $\int S_z ds=1$ W, where ds is differential area. Notice that the fields become more confined as ϵ_1 increases. Also, interestingly, there is negative power flow in the metal region outside the hole.

Circular waveguides in metal films have propagating modes for an arbitrarily small radius. As in 2D slots, small circular and, presumably, other aperture geometries can achieve resonant transfer through a metal film. While the loss increases with the reducing hole size, if the hole contains a material with an appreciable positive dielectric constant, the dominant mode can have modest loss over quite a wide wavelength range. This opens the opportunity for many applications which require small spatial resolution.

Support for related work came from the National Science Foundation (Contract Nos. 0203240-ECS and 0323037-ECS) and the Department of Energy Office of Nonproliferation and Research and Engineering (NA22), in conjunction with Lawrence Livermore National Laboratory.

*Electronic address: webb@purdue.edu

[1] T. W. Ebbesen, H. J. Lezec, H. F. Ghaemi, T. Thio, and P. A. Wolff, Nature (London) **391**, 667 (1998).
[2] H. F. Ghaemi, T. Thio, D. E. Grupp, T. W. Ebbesen, and H. J. Lezec, Phys. Rev. B **58**, 6779 (1998).
[3] A. Degiron, H. J. Lezec, W. L. Barnes, and T. W. Ebbesen, Appl. Phys. Lett. **81**, 4327 (2002).
[4] L. Martín-Moreno, F. J. García-Vidal, H. J. Lezec, A. Degiron, and T. W. Ebbesen, Phys. Rev. Lett. **90**, 167401 (2003).
[5] K. J. Klein Koerkamp, S. Enoch, F. B. Segerink, N. F. van Hulst, and L. Kuipers, Phys. Rev. Lett. **92**, 183901 (2004).
[6] T. Thio, K. M. Pellerin, R. A. Linke, H. J. Lezec, and T. W. Ebbesen, Opt. Lett. **26**, 1972 (2001).
[7] H. J. Lezec, A. Degiron, E. Devaux, R. A. Linke, L. Martin-Moreno, F. J. Garcia-Vidal, and T. W. Ebbesen, Science **297**, 820 (2002).
[8] W. L. Barnes, W. A. Murray, J. Dintinger, E. Devaux, and T. W. Ebbesen, Phys. Rev. Lett. **92**, 107401 (2004).
[9] A. Degiron, H. J. Lezec, N. Yamamoto, and T. W. Ebbesen, Opt. Commun. **239**, 61 (2004).
[10] E. N. Economou, Phys. Rev. **182**, 539 (1969).
[11] I. P. Kaminow, W. L. Mammel, and H. P. Weber, Appl. Opt. **13**, 396 (1974).
[12] B. Wang and G. P. Wang, Appl. Phys. Lett. **85**, 3599 (2004).
[13] J. Lindberg, K. Lindfors, T. Setälä, M. Kaivola, and A. T. Friberg, Opt. Express **12**, 623 (2004).
[14] L. Novotny and C. Hafner, Phys. Rev. E **50**, 4094 (1994).
[15] B. Prade and J. Y. Vinet, J. Lightwave Technol. **12**, 6 (1994).
[16] U. Schröter and A. Dereux, Phys. Rev. B **64**, 125420 (2001).
[17] H. A. Bethe, Phys. Rev. **66**, 163 (1944).
[18] I. A. Larkin, M. I. Stockman, M. Achermann, and V. I. Klimov, Phys. Rev. B **69**, 121403(R) (2004).
[19] P. B. Johnson and R. W. Christy, Phys. Rev. B **6**, 4370 (1972).
[20] E. D. Palik, *Handbook of Optical Constants of Solids* (Academic Press, San Diego, 1985).
[21] A. Yariv, *Optical Electronics* (Saunders College Publishing, Philadelphia, 1991).
[22] H. Shin, P. B. Catrysse, and S. Fan, Phys. Rev. B **72**, 085436 (2005).